

Optimization of high-order harmonic brightness in the space and time domains

Hyung Taek Kim,¹ I. Jong Kim,¹ Dong Gun Lee,¹ Kyung-Han Hong,¹ Yong Soo Lee,¹ Valer Tosa,² and Chang Hee Nam¹

¹*Department of Physics, KAIST, Yuseong-gu, Daejeon 305-701, Korea*

²*NIRDIMT, Donath 69-103, Cluj Napoca, Romania*

(Received 6 January 2004; published 23 March 2004)

Brightness of high-order harmonics is optimized in the space domain by profile flattening and self-guiding of intense femtosecond laser pulse and in the time domain by controlling the laser chirp. The profile flattening and self-guiding of the laser pulse propagating through a long gas jet effectively increased the phase-matched harmonic generation volume, thereby obtaining strong harmonics with low beam divergence, and the laser chirp control allowed the generation of spectrally sharp harmonics. At optimized conditions, the 61st harmonic, obtained at 134 Å from Ne, had a brightness of about 1×10^{15} W/cm²/srad with a beam divergence of 0.5 mrad and a spectral bandwidth of 0.7 Å.

DOI: 10.1103/PhysRevA.69.031805

PACS number(s): 42.65.Ky, 32.80.-t, 42.65.Wi, 52.38.-r

High-order harmonics emitted by noble gases, driven by intense laser field, have emerged as a unique source of extreme ultraviolet (EUV)/soft x rays, having features such as excellent coherence [1,2], ultrashort pulse duration [3], continuous wavelength tuning capability [4], and tabletop scale. For practical applications of such harmonic light sources to interferometry and ultrafast spectroscopy [5,6], the generation of bright high-order harmonics is very essential [7–10]. Strong high-order harmonic generation requires the application of intense femtosecond laser pulse to a high-density gas medium that is partially ionized during the harmonic generation process. The ionized gas medium, with higher electron density in the center than in the outer region, acts as a negative lens, leading to defocusing of the laser beam in a plasma and hence to a reduction in the effective harmonic generation volume [7,11]. In addition, the rapidly ionizing high-density gas medium modifies the temporal structure of the femtosecond laser pulse due to the self-phase modulation (SPM) [12]. Consequently, we have to optimize the harmonic generation conditions in both space and time domains in order to maximize the harmonic generation volume and to generate spectrally sharp harmonics, respectively.

In this Rapid Communication, we present experimental and theoretical results on the generation of bright harmonics using profile-flattened and chirp-controlled femtosecond laser pulses interacting with a long neon gas jet. The main advantages of harmonic generation in the long gas jet are the simplicity in target alignment and the capability of coupling large laser energy into large interaction volume; however, the plasma defocusing effect should be overcome in order to fully utilize the long medium. The plasma defocusing may be exactly compensated by tailoring the convergence of the laser beam entering the gas target. We directly measured profile flattening at the end of the gas medium, which induces self-guided laser propagation. This results in profile flattening and self-guiding of intense femtosecond laser pulses, which effectively increases the phase-matched harmonic generation volume. Simultaneously, harmonic spectrum was controlled by changing laser chirp with keeping guided laser propagation [13].

Profile flattening and self-guiding may occur when a converging laser beam compensates the plasma defocusing. When a gas medium is ionized by a laser pulse with a Gauss-

ian spatial profile (or any profile peaked at the center) and is positioned before the laser focus, the central part of the laser beam is refracted outwards due to higher electron concentration at the center, whereas the less-affected outer beam still converges. This redistributes the laser beam spatially so as to form a flattened profile in the central portion. After formation of the flat-top laser profile, the electron density profile is also flattened in the same region but changes rapidly at the boundary. This creates a flattened refractive index profile with a sharp increase at the boundary, which constitutes a wave guide in which the laser beam is self-guided. The profile flattening and self-guiding of intense laser pulse can significantly enhance the effective harmonic generation volume, thereby increasing the harmonic generation efficiency.

We first investigated the conditions for self-guided propagation of an intense femtosecond laser pulse through a long gas medium. Laser pulses of 27-fs duration and wavelength centered at 827 nm were focused using a spherical mirror ($f=1.2$ m) onto a long neon gas jet with a 9-mm slit nozzle. The peak gas density was about 40 Torr. The measured beam waist at the laser focus was $72 \mu\text{m}$ in full width at half maximum (FWHM), reaching a peak laser intensity of 2×10^{15} W/cm². To examine the laser propagation through the gas medium, visible plasma image and laser beam profile after the medium were recorded by charge-coupled-device (CCD) detectors. When the center of the gas jet nozzle was positioned at the laser beam focus, the gas jet position was defined as $z=0$.

We observed drastic changes in the laser propagation when the gas jet position was moved along the laser propagation direction. The visible plasma image was monitored from a transverse direction and the laser beam profile at the end of the medium was also obtained by imaging it on a CCD. Figure 1(a) shows two visible images of the plasma column obtained at the gas jet positions $z=0$ and -18 mm using negatively chirped 42-fs laser pulses of 5-mJ energy. The reason for using negatively chirped laser pulse will be given later. When the gas jet was positioned at $z=0$, the plasma image was bright only for the first 2-mm section of the gas medium due to the plasma defocusing effect. Though the Rayleigh length of the focused laser beam was longer than the length of the gas jet, the plasma defocusing severely limited the effective interaction length for harmonic genera-

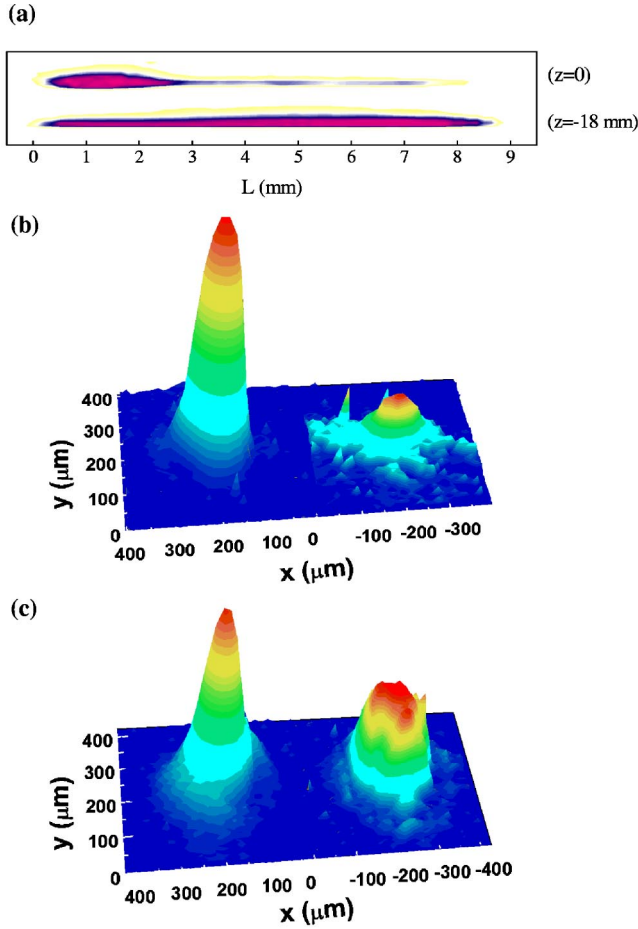


FIG. 1. (Color online) (a) Visible images of Ne plasma obtained at two gas jet positions $z=0$ and -18 mm. L is the propagation distance measured from the entrance of a 9-mm gas jet. Laser beam profiles at the entrance (left) and exit (right) of the gas jet for the cases of (b) $z=0$ and (c) $z=-18$ mm.

tion. This limitation occurs whenever strong, absorption-limited harmonic generation is attempted and, hence, a careful selection of a target location is essential to ensure a sufficiently long interaction length. As the gas jet was moved to a position before the laser focus, the bright part of plasma image got extended and a nearly uniform plasma column was generated along the entire length of the gas jet when located at $z=-18$ mm. This shows clearly that the self-guiding of the propagating laser pulse occurs at a properly selected target position.

The intensity profile of the laser beam at the exit position of the gas jet was directly measured using an image-relaying lens and a CCD. The intensity profile of the laser beam also had a strong dependence on the gas jet position. For the gas jet placed at $z=0$, the laser beam profile at the entrance position of the gas jet is shown in Fig. 1(b). After the propagation through the gas jet, the laser beam was almost spread out because it was severely defocused by the ionized medium, as also shown in Fig. 1(b). At the gas jet position of $z=-18$ mm, for which the self-guided propagation of the laser pulse occurred, flattening of the laser beam profile was observed as shown in Fig. 1(c). It clearly showed that the

laser intensity profile was flattened during guided propagation of laser beam. This profile flattened and self-guided propagation forms the uniform field distribution of laser pulses in space, which can provide an ideal condition for efficient, low-divergence harmonic generation.

Semiquantitative analysis of the profile flattening can be obtained from the analysis of the phase of the laser pulse propagating through an ionized medium. In the case of a focusing Gaussian beam, the phase $\phi(r, z)$ can be expressed, in terms of the coordinate of laser propagation z and radial coordinate r , as [14]

$$\phi(r, z) = k_0 \int_{z_0}^z n(r, z') dz' + \arg \left[\frac{1}{2(z_R + iz)} \exp \left(-\frac{k_0 r^2}{2(z_R + iz)} \right) \right], \quad (1)$$

where k_0 is the wave number in vacuum, z_0 is the position of the front face of the gas target, and z_R is the Rayleigh length. The main contribution to the refractive index n comes from free electrons and is given by $1 - N_e/2N_c$, where N_e is the electron density. The critical density N_c is defined as $N_c = m\epsilon_0\omega^2/e^2$, where m and e are the electron mass and charge, respectively, and ϵ_0 the vacuum dielectric constant and ω the laser frequency. The radial wave number can then be derived, assuming uniform refractive index along the z axis, as follows:

$$k_r = \frac{\partial}{\partial r} \phi = -k_0 \left[\frac{\rho(z - z_0)}{2N_c} \frac{\partial}{\partial r} P_e(r) - \frac{r}{R(z)} \right], \quad (2)$$

where $R(z) = z + z_R^2/z$ is the radius of curvature and ρ is the medium density. The ionization probability P_e is calculated from the Ammosov-Delone-Krainov model [15]. The radial wave number provides information of the propagation direction of the laser pulse along the radial axis. The laser pulse diverges (or converges) for positive k_r (negative k_r). If the central part of the laser pulse has positive k_r and outer part has negative k_r , the spatial profile of the laser pulse will be flattened up to the boundary defined by $k_r=0$. At this position, the first (ionization) term in Eq. (2) is balanced by the second (geometric) term, which forms the boundary of flattened profile.

For the case of $z=-18$ mm, the value of k_r , shown as the dotted line in Fig. 2, is evaluated corresponding to ionization at the pulse peak taking account of the entire gas medium. It is seen that k_r goes to zero at $r=62 \mu\text{m}$, which closely coincides with the boundary of the flattened laser beam profile shown as the solid line in Fig. 2. This analysis shows that the profile flattening was induced mainly by the plasma defocusing effect on a converging laser beam. In the case of neon, the self-focusing, due to the Kerr effect, is very small; hence, the plasma defocusing and convergence of the incident laser beam dominate the laser propagation. This simple model also yields the gas jet position for the maximum harmonic generation. Since the magnitude of the geometric term is maximum at $z=-z_R$ in Eq. (2), the placement of the target at that position allows the first term to attain its maximum, which corresponds to the maximum number of target atoms within

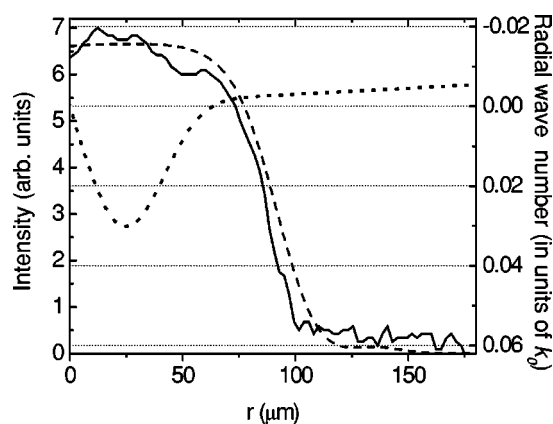


FIG. 2. Radial profile of the laser beam at the exit of the gas jet for the case of $z=-18$ mm, taken from the experimental result shown in Fig. 1(c) (solid line) and from the 3D simulation (dashed line). The dotted line refers to the radial wave-number profile calculated using Eq. (2).

the flattened beam cross section for a given laser intensity, thereby satisfying the condition for efficient harmonic generation.

To confirm the self-guided propagation of a profile-flattened laser pulse, we performed a three-dimensional (3D) simulation of femtosecond laser propagation by solving the wave equation for the conditions used in the experiment [16]. The simulation assumed radial symmetry and included effects related to the laser propagation such as diffraction, refraction, nonlinear self-focusing, ionization, and plasma defocusing. The results of simulation also revealed flattening of the beam profile in good agreement with the experimental results, shown by dashed line in Fig. 2. Therefore, the profile flattening clearly occurred in the self-guided propagation, which generated the bright harmonics.

We then investigated the spectral characteristics of high-order harmonics in the wavelength range of 120–180 Å. The harmonics generated from a long Ne gas jet were detected by a flat-field soft x-ray spectrometer equipped with a back-illumination x-ray CCD. Since the self-guiding condition of the laser pulse strongly depended on the gas jet position, the harmonic generation was also dramatically affected. We observed dramatic increase of harmonic signal as the gas jet was placed before the laser focus, as shown in Fig. 3. The 61st harmonic at 134 Å was the strongest among observed harmonics and at the gas jet position of $z=-18$ mm its spectral brightness was two orders of magnitude larger than that obtained at $z=0$. This position is close to the position $z=-z_R=-16$ mm estimated from Eq. (2) for efficient harmonic generation. At the optimum condition, the 61st harmonic was strong enough to saturate the x-ray CCD in a single shot of 5-mJ laser pulse. The beam divergence of the harmonics was measured by installing a cylindrical mirror in the soft x-ray spectrometer, instead of a toroidal mirror. The measured divergence of the 61st harmonic was 0.5 mrad (FWHM).

The self-guiding and profile flattening can provide a good phase matching between generated harmonics and a driving laser pulse. After the attainment of self-guided laser propagation, the geometric phase and the atomic phase do not

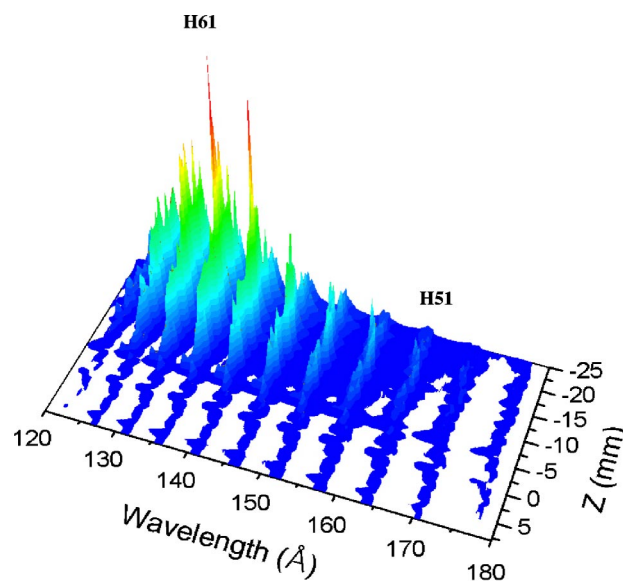


FIG. 3. (Color online). Generation of bright harmonics from Ne by adjusting the target position along the laser propagation direction. Bright harmonics were obtained around the 61st order by placing the target at 18 mm before the laser focus. “ H_n ” denotes the harmonic order.

affect the phase matching condition due to the collimated propagation and uniform intensity distribution of driving laser pulses. In this case the dispersion, contributed mainly by the neutral atoms and free electrons, determines the phase-matching condition. The peak laser intensity estimated from the spatial profile shown in about Fig. 2 is 6×10^{14} W/cm². The 61st harmonic satisfies the phase-matching conditions at the ionization level of about 1%. The 3D simulation showed that this ionization level occurred at the leading edge of the laser pulse after the profile flattening was developed. The profile flattening automatically overcomes the problems associated with the variation of phase-matching conditions along the radial direction, leading to a larger effective volume for harmonic generation. As the gas density and length corresponds to six times the absorption length in Ne, the generated harmonics are limited by the absorption in Ne. Consequently, the self-guiding and profile flattening provided an ideal condition for well phase-matched strong harmonic generation in a large volume. In addition, the use of profile-flattened laser pulses can be beneficial in resolving the spatial chirp problem [17] for the attosecond pulse generation because of the flattened laser intensity profile.

The spectral sharpness can be controlled by adjustment of the laser chirp. Even though the arrangement of the gas jet at 18 mm before the laser focus optimized the harmonic generation in the space domain, the harmonic spectrum can be broadened by the frequency chirp of harmonics [13]. Figure 4 shows the chirp dependence of harmonic spectra with the Ne gas jet at $z=-18$ mm. The laser chirp was controlled by changing the grating separation in the pulse compressor while keeping the laser energy fixed. The negatively chirped 42-fs pulse generated the sharpest and brightest harmonics while the positively chirped 41-fs pulse produced a quasi-continuous harmonic spectrum. The laser propagation condi-

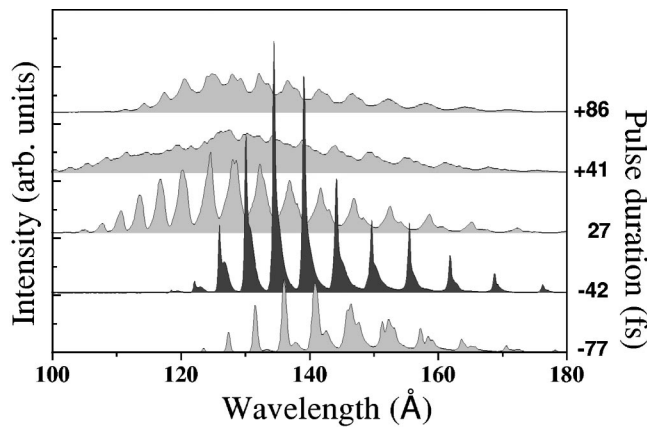


FIG. 4. Harmonic spectra from Ne driven by femtosecond laser pulses with different laser chirp. The sign of the pulse duration refers to the sign of applied laser chirp.

tions did not depend sensitively on the sign of the laser chirp. The 3D simulation showed that the guided laser intensity was slightly higher in the case of the chirp-free 27-fs pulse than that in the case of negative 42-fs pulse. In the case of a rapidly ionizing high-density medium, the harmonic chirp is dominated by the SPM-induced positive chirp in the leading edge of the laser pulse [12,13]. As a result, a negatively chirped laser pulse can compensate the SPM-induced positive chirp and generate sharp and bright harmonics. With the negatively chirped 42-fs pulse, the bandwidth of the 61st harmonic was 0.7 \AA and the spectral brightness was enhanced four times over that obtained from a chirp-free 27-fs pulse. Consequently, we have achieved simultaneous optimization of bright harmonic generation in space and time using the self-guided and chirped femtosecond laser pulses.

The energy calibration was performed to estimate the brightness of 61st harmonic. At the optimum condition, the energy of the 61st harmonic was estimated to be 0.4 nJ, measured using a EUV silicon photodiode (International Radiation Detectors AXUV-100) in place of the x-ray CCD but assuming nominal values of grating diffraction efficiency, reflectivity of the toroidal mirror, quantum efficiency of the EUV photodiode. This is a very conservative estimation, considering oxidation and contamination of optical components and detector with time. The harmonic brightness, defined as the power of a harmonic per unit area per unit solid angle subtended at the source, was estimated to be about $1 \times 10^{15} \text{ W/cm}^2/\text{srad}$ (also a conservative value), which is more than an order of magnitude larger than that reported by Nisoli *et al.* [8] obtained using a truncated Bessel beam.

In conclusion, profile flattening and self-guiding of intense femtosecond laser pulse, achieved by placing a gas target before the laser focus, and the laser chirp control led to the generation of bright harmonics with low beam divergence. We found that the plasma defocusing effect severely limited the effective interaction length of harmonic generation and a proper selection of target position resulted in the self-guiding of profile-flattened laser pulse, providing efficient harmonic generation. This achievement of high brightness high-order harmonics with narrow spectral bandwidth will be useful for various applications of harmonic EUV/soft x-ray sources. With the availability of high reflectivity of Mo:Si mirrors at 134 \AA , corresponding to the wavelength of the strong 61st harmonic from Ne, the current results will be valuable, especially for the metrology in future EUV lithography optics.

This research was supported by the Ministry of Science and Technology of Korea through the Creative Research Initiative Program.

-
- [1] R. A. Bartels, A. Paul, H. Green, H. C. Kapteyn, M. M. Murnane, S. Backus, I. P. Christov, Y. Liu, D. Attwood, and C. Jacobson, *Science* **297**, 376 (2002).
- [2] D. G. Lee, J. J. Park, J. H. Sung, and C. H. Nam, *Opt. Lett.* **28**, 480 (2003).
- [3] M. Paul, E. S. Toma, P. Breger, G. Mullot, F. Audebert, Ph. Balcou, H. G. Muller, and P. Agostini, *Science* **292**, 1689 (2001).
- [4] H. T. Kim, D. G. Lee, K.-H. Hong, J.-H. Kim, I. W. Choi, and C. H. Nam, *Phys. Rev. A* **67**, 051801(R) (2003); H. J. Shin, D. G. Lee, Y. H. Cha, K. H. Hong, and C. H. Nam, *Phys. Rev. Lett.* **83**, 2544 (1999).
- [5] M. Drescher, M. Hentschel, R. Kienberger, M. Uiberacker, V. Yakovlev, A. Scrinzi, Th. Westerwalbesloh, U. Kelleneberg, U. Heinzmann, and F. Krausz, *Nature (London)* **419**, 803 (2002).
- [6] L. Nugent-Glandorf, M. Scheer, D. A. Samuels, A. M. Mulhisen, E. R. Grant, X. Yang, V. M. Bierbaum, and S. R. Leone, *Phys. Rev. Lett.* **87**, 193002 (2001).
- [7] D. G. Lee, H. T. Kim, K.-H. Hong, and C. H. Nam, *Appl. Phys. Lett.* **81**, 3726 (2002).
- [8] M. Nisoli, E. Priori, G. Sansone, S. Stagira, G. Cerullo, S. De Silvestri, C. Altucci, R. Bruzzese, C. de Lisio, P. Villoresi, L. Poletto, M. Pascolono, and G. Tondello, *Phys. Rev. Lett.* **88**, 033902 (2002).
- [9] E. Takahashi, Y. Nabekawa, T. Otsuka, M. Obara, and K. Midorikawa, *Phys. Rev. A* **66**, 021802(R) (2002).
- [10] S. Kazamias, D. Douillet, F. Weihe, C. Valentin, A. Rousse, S. Sebban, G. Grillon, F. Augé, D. Hulin, and Ph. Balcou, *Phys. Rev. Lett.* **90**, 193901 (2003).
- [11] M. Bellini, C. Corsi, and M. C. Gambino, *Phys. Rev. A* **64**, 023411 (2001).
- [12] J.-H. Kim and C. H. Nam, *Phys. Rev. A* **65**, 033801 (2002).
- [13] D. G. Lee, J.-H. Kim, K.-H. Hong, and C. H. Nam, *Phys. Rev. Lett.* **87**, 243902 (2001).
- [14] A. E. Siegman, *Lasers* (University Sciences, Mill Valley, CA, 1986), p. 640.
- [15] M. V. Ammosov, N. B. Delone, and V. P. Kraïnov, *Zh. Eksp. Teor. Fiz.* **91**, 2008 (1986) [*Sov. Phys. JETP* **64**, 1191 (1986)].
- [16] V. Tosa, E. Takahashi, Y. Nabekawa, and K. Midorikawa, *Phys. Rev. A* **67**, 063817 (2003).
- [17] M. B. Gaarde and K. J. Schafer, *Phys. Rev. Lett.* **89**, 213901 (2002).